EXPLORING LUNAR GRABEN FORMATION WITH DISPLACEMENT-LENGTH SCALING. E. S. Martin[1] and T. R. Watters[1] [1]Center for Earth and Planetary Studies, National Air and Space Museum, Smithsonian Institution (martines@si.edu).

Introduction: Lunar nearside graben often form radial and/or concentric to mare basins. The formation of these graben have been attributed to mascon tectonics [1, 2, 3, 4]. Mascon tectonics predict the presence of concentric and/or radial graben on the edges of mascon mare, and radial and/or concentric wrinkle ridges within the mare [1, 2, 3, 4, 5]. Non-mascon mare show similar tectonic patterns, attributed to the loading of a thinner and/or weaker lithosphere by mare basalts [6]. To further our understanding of nearside graben formation, we use maximum displacement-length scaling relations [e.g. 7, 8, 9] of the normal faults that are influenced by the mechanical properties and tectonic setting of deformed crustal materials.

Data Collection: Thirty graben were selected for this work. We selected graben that were not significantly degraded and could be traced along most of their lengths. Graben were sampled across multiple terrains highlands, mare, and mixed (mare and highlands). For each graben, we determined its total length and maximum displacement.

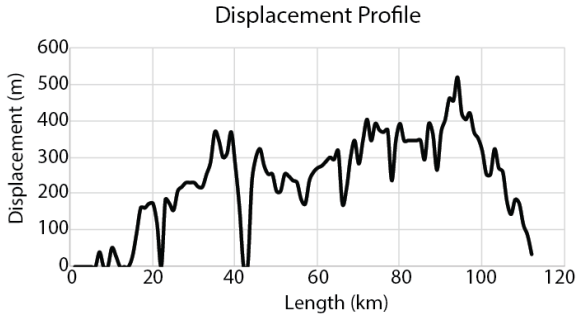

Fig. 1: *A graben displacement profile used to identify a graben's length and maximum displacement (D_{max}).*

Displacement. The throw on graben bounding normal faults was measured at 1 km intervals using LOLA-SELENE gridded data [10]. Displacement was inferred from throw assuming an average fault dip of 60°. A displacement profile (Fig. 1) was created for each of the graben bounding normal faults to assess which fault experienced the greatest displacement.

Maximum Displacement. Displacement profiles provide a robust means to determine a fault's maximum displacement and its location on the fault. From linear fracture mechanics [e.g. 7], a fault should achieve its maximum displacement near the midpoint along length and zero displacement at the fault tips. Maximum displacement will not necessarily always occur at the fault-length midpoint. Displacement profiles allow the location of D_{max} and the shape of the profile to be evaluated (Fig. 1).

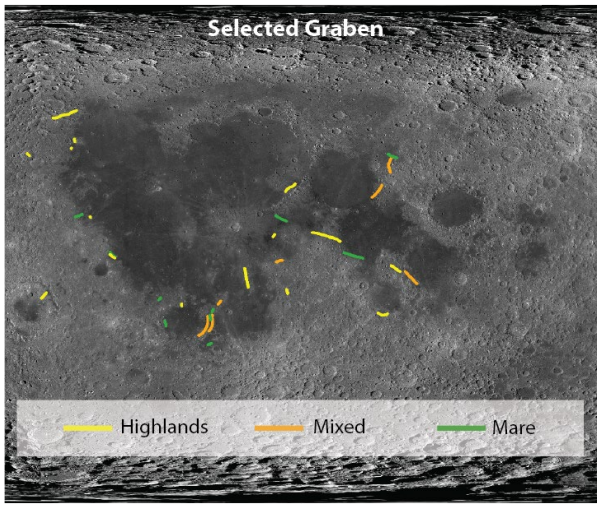

Fig. 2: *Distribution of selected nearside graben color coded by terrain.*

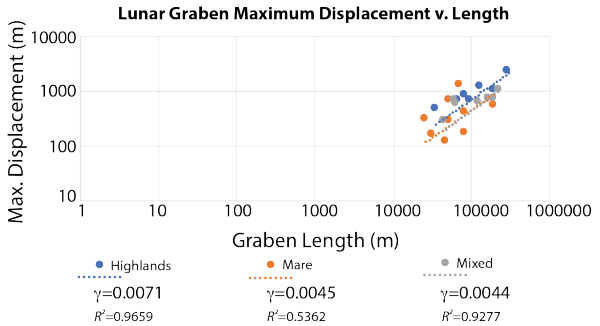

Fig. 3: *Displacement-length scaling of three populations of lunar nearside graben selected in this study e.g. Fig. 2.*

Results: We find values of γ, determined by a linear fit to the D_{max}/L ratio of the population of examined normal faults, for graben in the highlands is γ=0.0071, for graben in the mare is γ=0.0044, and for graben in mixed environment is γ=0.0045 (Fig. 3). Each graben population shows some scatter, quantified by the R^2 value (Fig. 3) of each least squares fit trendline. Mare graben have the greatest amount of scatter, with an R^2=0.536, and highlands and mixed graben the least (R^2=0.966 and R^2=0.928 respectively).

Discussion: On Earth, the average global estimate for γ for all fault populations is 0.01 [11] with most terrestrial faults falling between γ=0.1 and γ=0.001 (Fig. 4). Lunar graben from this study fall within this range (Fig. 4) and are consistent with previous *D-L* scaling studies of graben on the Moon [12]. The values of γ for the populations of lunar graben are generally lower than that of terrestrial normal faults (Fig. 4). Rheology can play a role in variations of γ in fault populations, although this may not always be the controlling factor. For example, basaltic environments on Earth have γ=0.003 for an Icelandic Holocene rift [13] and γ=0.007-0.008 for the East Pacific Rise [14, 15]. The values of γ for terrestrial basaltic environments span a similar range of γ values for our population of lunar graben γ=0.0044-0.0071. While useful to understand how fault populations across the solar system compare, the strain environment on Earth differs from one-plate planetary bodies like the Moon. We therefore interpret the difference in γ for graben on the Moon to be largely due to the difference in the strain regime.

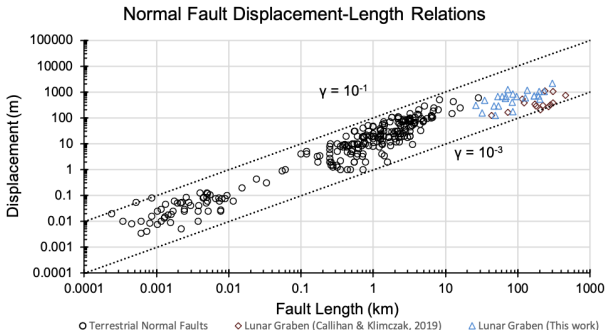

Fig. 4: *Displacement-length scaling for terrestrial normal faults [7, 16] compared and lunar graben in this work, and from [12].*

We further consider the influence of mare basalts on lunar graben by looking at the scatter in a graben population. We use the R^2 value of the least squares fit trendline to evaluate the scatter in population of mare graben. Typically, scatter in γ may be the result of many factors including rock property variations and fault linkage/interactions [11]. We interpret the large scatter (R^2=0.536) in the mare graben population to be the result of variation in thickness of the mare basalt sequences that is influencing the growth of the normal faults. The variability in the mare data suggests that normal fault growth may be restricted by the local thickness of the mare basalts.

It is interesting to note that the R^2 value for mixed environment graben (0.928) indicates less scatter than found in the mare basalt normal fault data while having a nearly identical γ value for the populations. The smaller scatter in the mixed environment, indicated by the R^2 value, may suggest that unrestricted normal fault growth in a mechanically unstratified highlands is the controlling influence rather than the local thickness of the mare basalts.

Future work will consider displacement profiles of graben looking for irregular profile shapes that may be associated with fault linkages that could account for some of the scatter of the mare graben population [11]. Further assessment of the shape of displacement profiles of normal faults of mare graben will also be compared with those of highlands and mixed graben populations to look for further evidence of restricted fault growth.

Acknowledgments: We acknowledge the hard work of the LROC team in data acquisition, distribution, and support. We also acknowledge the LRO engineers and technical support personnel. This work was supported by the LRO project and an ASU LROC contract to TRW.

References: **[1]** Melosh, H. J. (1978) *9th LPSC* p. 3513-3525. **[2]** Solomon & Head (1979), *JGR,* 84, 1667-1682. **[3]** Solomon & Head (1980), *Review of Geophysics,* 18, 107-141. **[4]** Freed et al., (2001) *JGR* 106, 20603-20620. **[5]** Watters et al., (2015) *Geology*, 42, 851-854. **[6]** Martin & Watters (2021), *Icarus, 354,* 114039. **[7]** Cowie & Scholz (1992a), *J. Struct. Geol, 14* 1133-1148. **[8]** Cowie & Scholz (1992b), *J. Struct. Geol. 14,* 1149-1156. **[9]** Schultz et al (2010), *Planetary Tectonics,* p. 457. **[10]** Barker et al (2016), *Icarus 273,* 346-355. **[11]** Cowie, (1998), *Geophysical Monograph Series,* v. 106 p. 325-348. **[12]** Callihan & Klimczak (2019), *Lithosphere,* 11, 294-305. **[13]** Gudmundsson (1992), *Terra Nova, 4*, 464-471. **[14]** Cowie et al. (1994), *J. Geophys. Res, 98,* 17911-17920. **[15]** Carbotte & Macdonald (1994), *JGR, 99*, 13609-13631. **[16]** Watters et al. (2000), *GRL, 27*, 3659-3662.